Distributions of γ-Aminobutyric Acid Immunoreactive and Acetylcholinesterase-Containing Cells in the Primary Olfactory System in the Terrestrial Slug Limax marginatus

Authors: Ito, Iori, Watanabe, Satoshi, Kimura, Tetsuya, Kirino, Yutaka, and Ito, Etsuro

Source: Zoological Science, 20(11) : 1337-1346

Published By: Zoological Society of Japan

URL: https://doi.org/10.2108/zsj.20.1337

ZOOLOGICAL SCIENCE **20**: 1337–1346 (2003)

Distributions of γ-Aminobutyric Acid Immunoreactive and Acetylcholinesterase-Containing Cells in the Primary Olfactory System in the Terrestrial Slug *Limax marginatus*

Iori Ito[1,2], Satoshi Watanabe[2], Tetsuya Kimura[3], Yutaka Kirino[2], and Etsuro Ito[1,4*]

[1]*Laboratory of Animal Behavior and Intelligence, Division of Biological Sciences, Graduate School of Science, Hokkaido University, Sapporo 060-0810, Japan*
[2]*Laboratory of Neurobiophysics, Graduate School of Pharmaceutical Sciences, The University of Tokyo, Tokyo 113-0033, Japan*
[3]*Brain-Operative Expression Laboratory, Brain Science Institute, Riken, Wako 351-0198, Japan*
[4]*Division of Innovative Research, Creative Research Initiative "Sousei" (CRIS), Hokkaido University, Sapporo 001-0020, Japan*

ABSTRACT—The tentacular ganglion, the primary olfactory system of terrestrial slugs, exhibits spontaneous oscillations with a spatial coherence. The digit-like extensions (digits) of the tentacular ganglion presumably house the cell bodies of the neurons underlying the oscillations. The present study was designed to identify the anatomical and physiological determinants of these oscillations with a special focus on whether the neurons located in the digits contribute to the coherent oscillations. We recorded field potentials from the spatially separated sites in the digits in the terrestrial slug *Limax marginatus*. We also simultaneously recorded tentacular nerve to monitor the coherent oscillations. The spatially separated regions in the digits oscillated at the same frequency as the tentacular nerve, indicating a single coherent activity. To study the neural networks underlying the coherent oscillations, we examined the distributions of acetylcholinesterase (AChE)-containing and γ-aminobutyric acid immunoreactive (GABA-ir) neurons. AChE-containing and GABA-ir fibers were found to connect the neurons in a branch of the digits with those in other branches. We also used a vital staining technique with 1,1'-didodecyl-3,3,3',3'-tetramethylindocarbocyanine perchlorate to examine the projections of neurons in the digits. Large stained cells were detected in many branches of the digits after placing the dye on one of the cell masses located in right and left sides of the tentacular ganglion. They were detected in the cell masses and in many branches of the digits after placing the dye on a branch of the digits. Our results showed that the slug primary olfactory system has highly interconnected neural networks.

Key words: acetylcholine, mollusk, olfactory processing, tentacular ganglion

INTRODUCTION

Robust spontaneous oscillations and spatial coherence are common features of peripheral and central olfactory systems in the terrestrial slugs. The primary olfactory system (the tentacular ganglion) exhibits two types of oscillatory states with low (1.5 Hz fast oscillations) and high (0.5 Hz slow oscillations) spatial coherences in *Limax marginatus* (Inokuma *et al*., 2002). Odors greatly decrease the amplitude of the slow oscillations. This effect suggests that the coherent oscillations are involved in the first stage of the olfactory processing. The central olfactory system (the procerebral [PC] lobe), exhibits rhythmic propagating waves at 0.7 Hz (Gelperin and Tank, 1990), and odors transiently collapse the phase gradient of the propagating waves along the

* Corresponding author: Tel. +81-11-706-2615;
FAX. +81-11-706-4448.
E-mail: eito@sci.hokudai.ac.jp

lobe (Delaney *et al*., 1994). These results indicate that the coherent oscillations play an important computational role in olfactory processing from the peripheral to central olfactory systems.

The presence of the coherent oscillations in the tentacular ganglion suggests that highly interconnected networks are located in the tentacular ganglion as well as in the PC lobe. The tentacular ganglion is comprised of the neuropil region and spatially discrete units termed digits (Ito *et al*., 1999; Hatakeyama *et al*., 2001). Coherent oscillations can be recorded from the neuropil region of the tentacular ganglion (Inokuma *et al*., 2002). The digits ramify from the apical part of the tentacular ganglion into many thin neuropils and connect the neuropil region with the sensory epithelium. The surface of the digits is covered with a number of neuronal cell bodies including olfactory receptor neurons and olfactory interneurons (Chase and Kamil, 1983; Chase and Tolloczko, 1993; Ito *et al*., 2000). The digits can be divided into three major groups (right, central, and left groups), and two of them (left and right groups) have cell clusters, termed the cell masses, at their bases (Ito *et al*., 1999). The coherent oscillations may be produced by neurons in the digits and cell masses for the following two reasons. *(1)* The cell layer of the neuropil region of the tentacular ganglion contains only a small number of neurons (Ito *et al*., 2000). *(2)* The coherent oscillations change in response to odors (Ito *et al*., 2001). These anatomic and physiological features suggest that the olfactory neurons in the digits play a role in the coherent oscillations. However, the relationship between the local field potential (LFP) of the digits and that of the tentacular nerve has not yet been characterized.

Olfactory receptor neurons and some projection neurons in the antennal lobe of the sphinx moth *Manduca sexta* exhibit acetylcholinesterase (AChE) activity (Homberg *et al*., 1995). Although acetylcholine can alter the dynamics of the spontaneous oscillations in the PC lobe (Iwama *et al*., 1999; Watanabe *et al*., 2001), no histochemical studies on the distribution of the AChE-containing neurons in the primary and central olfactory systems in slugs have been performed. Recent studies from our laboratory have shown that picrotoxin, which is an antagonist of γ-aminobutyric acid (GABA) in *Lymnaea* neurons (Rubakhin *et al*., 1996) and in locust neurons (Stopfer *et al*., 1997), decreases the amplitude of oscillatory activity in the tentacular nerve, which carries afferent signals to the PC lobe in *L. marginatus* (Ito *et al*., 2001). Although GABAergic local neurons play an important role in synchronizing the olfactory projection neurons in locust (Stopfer *et al*., 1997), there are no studies that examined the distribution of GABAergic neurons in the primary olfactory system in slugs.

In the present study, we recorded the LFPs from the digits to examine the spatial coherency of the oscillations. We then applied an immunohistochemical technique to examine the distribution of GABAergic neurons and used a histochemical technique to examine the distribution of AChE-containing neurons in the primary olfactory system and the central nervous system (CNS) in the terrestrial slug *L. marginatus*. We analyzed the distributions of the GABAergic and cholinergic fibers to map the fiber networks that connect different groups of the digits and tentacular ganglia. We further used the vital staining technique of 1,1'-didodecyl-3,3,3',3'-tetramethylindocarbocyanine perchlorate (DiI) to study the projections of the neurons in the digits and cell masses in the primary olfactory system. The results showed that the primary olfactory system generates spatially coherent neural oscillations at 1–2 Hz and have highly interconnected neural networks.

MATERIALS AND METHODS

Animals

The terrestrial slugs *L. marginatus,* maintained in our laboratory on a 12:12 light:dark cycle at 19°C and fed on a paste of rat chow, were obtained either from our laboratory colony or collected in the open field.

Electrophysiological recording

Slugs were anesthetized by injection of 0.2–0.3 ml of an anesthetizing solution (see Kimura *et al*., 1998 for composition). The CNS with the attached superior and inferior tentacles were dissected out in a dish filled with a dissection solution consisting of (in mM) 35 NaCl, 2 KCl, 4.9 $CaCl_2$, 28 $MgCl_2$, 5 glucose, and 5 HEPES (pH 7.6). The connective tissue was removed with fine scissors. The tentacular nerve was cut at about 400 μm from the ganglion. A pair of electrodes was placed on two recording sites in the ventral surface of the central and left groups of the digits. The oscillations in the tentacular ganglion and tentacular nerve were recorded from the center of the ventral surface and the cut-end, respectively. Neural activity was led to a high-impedance probe (JB-101J, Nihon Kohden, Tokyo, Japan) and an AC amplifier with a 0.5 Hz to 1 kHz bandpass filter (Bioelectric Amplifier MEG-1200, Nihon Koden). The recording chamber was perfused continuously with *Limax* saline (see Kimura *et al*., 1998 for composition) at 1.5 ml/min.

Data analysis

Signal analyses were carried out off-line with custom-made programs developed with MATLAB (ver. 6.5.0.180913a; The MathWorks, Natick, MA, USA). To obtain sliding-window auto/cross-correlations between two recording sites in the digits (left and central groups of digits) and the tentacular nerve, the recording was divided into 10-s epochs and then the correlation function for the epoch was calculated.

GABA immunohistochemistry

The superior and inferior tentacles were fixed with 4% paraformaldehyde in 0.1 M phosphate buffer (PB; pH 7.4) for 24 hr at 4°C. Serial longitudinal cryostat sections (20 μm in thickness) were obtained as described previously (Fujie *et al*., 2002) and washed in PB containing 1% Triton X-100 for 3 hr at room temperature. Endogenous peroxidase activity was inhibited with a solution of 0.3% H_2O_2 and 0.1% sodium azide for 10 min. The sections were incubated with a primary anti-GABA antibody (Incstar, Stillwater, MN, USA) plus 10% goat serum diluted 1:1,000 with PB containing 1% Triton X-100 for 2 days at 4°C. After rinsing in PB, the sections were processed with an avidin-biotin immunoperoxidase method using an avidin-biotin-peroxidase complex (Vector Laboratories, Burlingame, CA, USA). Sections were examined under a light microscope (MICROPHOT-FXA, Nikon, Tokyo, Japan). No stainings were observed in the control experiment using the same procedure without the primary anti-GABA antibody. To count the num-

ber of stained cells, all sections from the right inferior tentacle that stained well were used.

AChE histochemistry

The preparations were fixed in 4% paraformaldehyde in PB for 3 hr. Serial longitudinal cryostat sections (20-μm thick) were

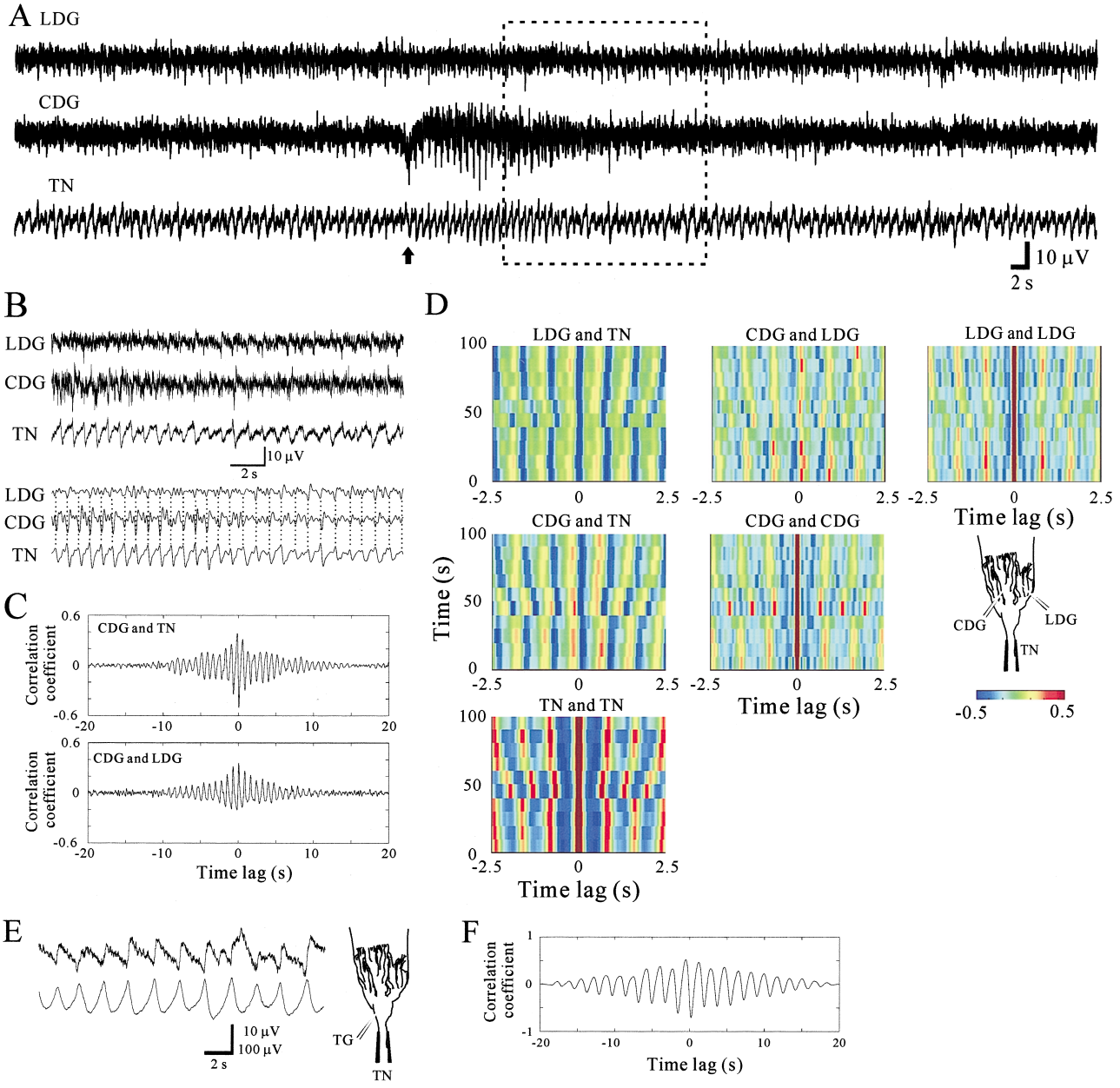

Fig. 1. Spontaneous coherent oscillations in the primary olfactory system of *Limax*. A. LFP signals of the spontaneous oscillations of the left (top) and central (middle) groups of the digits and tentacular nerve (bottom). The signal was digitally filtered with a band pass filter (0.1–30 Hz). An arrow indicates the onset of spontaneous frequency fluctuation. B. Magnified view of the LFP signal indicated by the box in A. The lower 3 traces are the same signals as above with a narrow band pass filter (0.6–2.4 Hz). Note that the polarity of the LFP signals in the digits is opposite to that in the tentacular nerve. C. Cross-correlations between the central group of the digits and tentacular nerve (the upper plot) and between the central and left groups (the lower plot) calculated from the signals shown in A. D. Sliding-window cross-correlations between a pair of the recording sites in the digits and tentacular nerve and sliding-window auto-correlations. The traces shown in A were divided into time epochs (10 s each). The auto-, cross-correlation functions were calculated for all time epochs. The correlation coefficient in each epoch was assigned a color to form an intensity-coded bar. These intensity-coded bars were stacked to visualize the changes in the auto-, cross-correlation functions. Time runs along the longitudinal-axis. The time lag of the correlation function runs along the horizontal-axis. Note that the auto-correlations of the central group of the digits are very similar to those of the tentacular nerve. A schematic drawing of the recording sites is shown on the right side. E. LFP signals (20 s) of the spontaneous oscillations of the tentacular ganglion (top) and tentacular nerve (bottom). A schematic drawing of the recording sites is shown on the right side. F. Cross-correlations between tentacular ganglion and tentacular nerve calculated from the signals shown in E. LDG, left group of the digits; CDG, central group of the digits; TN, tentacular nerve; TG, tentacular ganglion.

obtained as described previously (Fujie *et al*., 2002). We used the direct staining technique of Homberg *et al*. (1995). The sections were incubated for 30 min at room temperature in a diluted solution of original Karnovsky and Roots medium containing 180 μM acetylthiocholine iodide, 500 μM sodium citrate, 300 mM cupric sulfate, 50 μM potassium ferricyanide and 30 mM tetraisopropylpyrophosphoramide (iso-OMPA, an inhibitor of nonspecific cholinesterase) diluted in maleate buffer (0.1 M, pH 6.0) containing 0.5% Triton X-100. After rinsing the sections in 50 mM Tris-HCl buffer at pH 7.6, the cytochemical staining was intensified using the method described by Tago *et al*. (1986). The sections were examined under a light microscope (MICROPHOT-FXA, Nikon). One section that included the sensory epithelium, digits, cell mass and tentacular ganglion was used to estimate the ratio of each type of the AChE-containing cells.

Vital staining with DiI

The method of vital staining was based on the procedure described by Gelperin and Flores (1997). Briefly, crystals of DiI-C_{12}-(3) (# D-383, Molecular Probes, Eugene, OR, USA) formed on the tips of glass microelectrodes were placed on the third branch (counted from the tentacular ganglion) of the central group of the digits or in the left or right side of the cell mass. The preparations were incubated in *Limax* saline for ≥24 hr, fixed in 10% formalin, and mounted in PB. Images were acquired using an inverted microscope (IX-70; Olympus, Tokyo) equipped with a cooled CCD camera (ORCA-ER, Hamamatsu Photonics, Hamamatsu, Japan). Confocal images were acquired using a confocal laser scanning microscope (LSM 510; Carl Zeiss, Germany).

RESULTS

Cross-correlation analysis of spontaneous oscillations in the digits and tentacular nerve

We simultaneously recorded from three sites (the tentacular nerve and two spatially separated sites in the digits) and analyzed the signals in terms of correlation function. The cross-correlation function among these sites changed

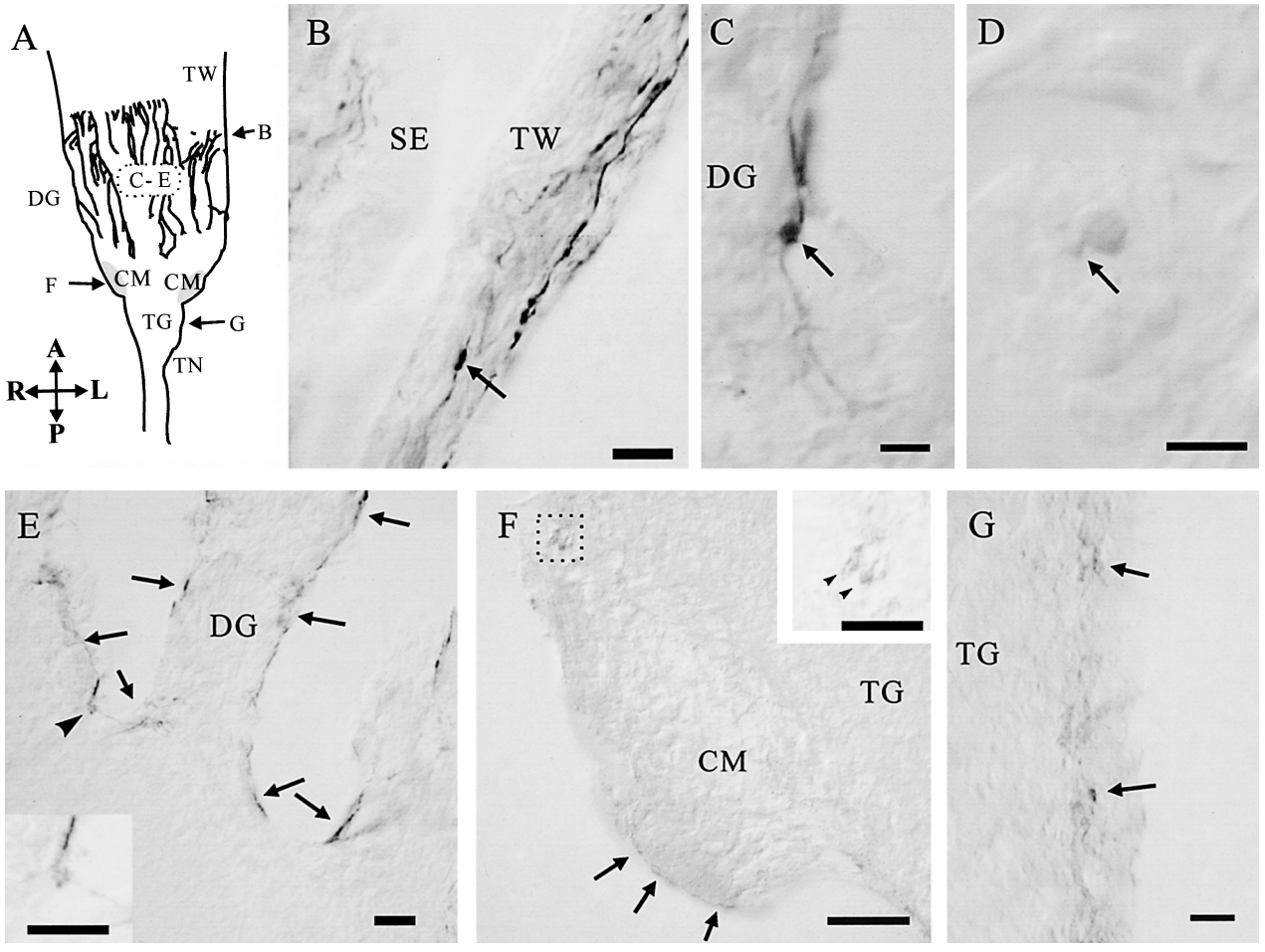

Fig. 2. Distribution of GABA immunoreactivity in the digits and tentacular ganglion. A. Schematic drawing of the retracted form of tentacle. Magnified positions are marked by alphabets. B. A stained bipolar cell body (arrow) in the tentacular wall of the right superior tentacle. C. A stained round bipolar cell (arrow) in the digits of the right inferior tentacle. D. A stained monopolar cell with round cell body in the digits of the right superior tentacle. An arrow shows a neurite. E. Stained fibers (arrows) running near the edge of the digits of the right superior tentacle. An arrowhead shows a stained cell body. The stained cell bodies are magnified in the inset. F. Stained cell bodies (box) and fibers (arrows) in the right cell mass of the right inferior tentacle. The two stained cell bodies in the box are magnified in the inset. Arrowheads show cell bodies. G. Stained cell bodies (arrows) in the tentacular ganglion of the right inferior tentacle. Calibration: B, 20 μm; C, 10 μm; D, 5 μm; E–G, 20 μm; insets in E, F, 20 μm. All sections of the tentacles were viewed from the ventral side. TW, tentacular wall; DG, digits; CM, cell mass; TG, tentacular ganglion; A, anterior; P, posterior; L, left; R, right; TN, tentacular nerve; SE, sensory epithelium.

sometimes dynamically with time. For example, the traces showed a transient increase in the frequencies of the central group of the digits and tentacular nerve (Fig. 1A). The negative peaks of the field potential oscillations in the central group of the digits correlated well with the positive peaks of those in the tentacular nerve during the first half of the traces (Fig. 1B). Then, the negative peaks of the field potential oscillations in the left group of the digits gradually became correlated with the positive peaks of those in the tentacular nerve. Because the polarity of oscillations in the digits was opposite to that in the tentacular nerve, the cross-correlation between the central group of the digits and the tentacular nerve had a minus peak at time lag 0 (Fig. 1C, top). The cross-correlation functions between the central and left groups of the digits showed a coherent component at the same frequency to the tentacular nerve oscillations (Fig. 1C, bottom). Sliding-window auto/cross-correlations also showed that the oscillations in the digits and the tentacular nerve were well correlated to each other (Fig. 1D).

Next, we recorded simultaneously from the two recording sites (the tentacular ganglion and tentacular nerve). The negative peaks of the field potential oscillations in the tentacular ganglion were also well correlated with the positive peaks of those in the tentacular nerve (Fig. 1E). The cross-correlation between the tentacular ganglion and tentacular nerve had a minus peak at time lag 0 (Fig. 1F). These results suggest that the primary olfactory system of *L. marginatus* has highly interconnected neural networks that produce the coherent oscillations. To examine the neuronal components of the networks underlying the coherent oscillations, we performed three histological analyses described below.

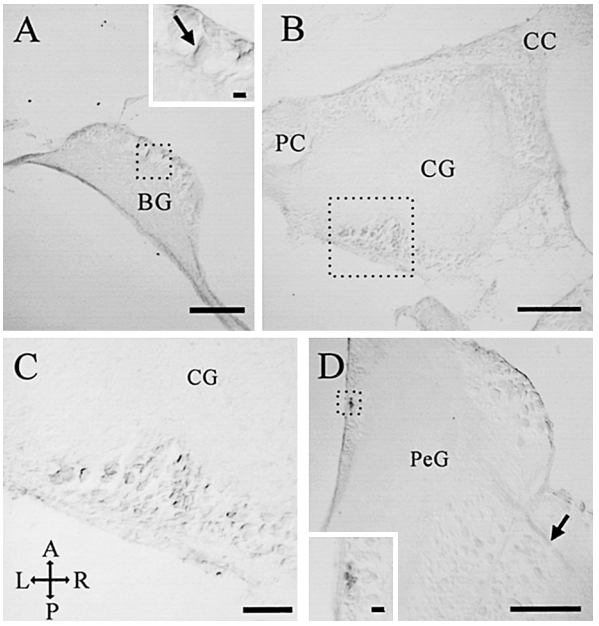

Fig. 3. Distribution of GABA immunoreactivity in the CNS. A. A stained cell body (arrow) in the right buccal ganglion. Magnified view is shown in the inset. B. A stained cell cluster in the left cerebral ganglion. C. Magnified view of the stained cells in the box in B. D. A stained cell cluster (box) and a fiber bundle (arrow) in the left pedal ganglion. The cell cluster is magnified in the inset. Calibration: A, B, 200 μm; C, 100 μm; D, 200 μm; insets in A and D, 20 μm. BG, buccal ganglion; CG, cerebral ganglion; PC, procerebral lobe; CC, cerebral commissure; A, anterior; P, posterior; R, right; L, left; PeG, pedal ganglion.

Distribution of GABA immunoreactive cells

GABA immunoreactivity was detected in the tentacular wall, digits, cell masses, and tentacular ganglion (Fig. 2). GABA immunoreactive (GABA-ir) cells in the tentacular wall were bipolar cells with sharp cell bodies (Fig. 2B). GABA-ir cell bodies with long axis of 3-5 μm were found in the cell layer of the digits (Fig. 2C–E). They had round (Fig. 2C, D) cell bodies and one (Fig. 2D) or two neuronal processes (Fig. 2C, E). These neuronal processes ran through the cell layers of the digits (Fig. 2C) and sometimes turned into the neighboring digit (small arrows in Fig. 2E). GABA-ir cell bodies with long axis of 3–6 μm were found in the cell masses (Fig. 2F). The GABA-ir fibers ran near the edge of the cell masses (arrows in Fig. 2F). GABA-ir cell bodies with long axis of 5–7 μm were found in the cell layer of the neuropil region of the tentacular ganglion (Fig. 2G). No GABA-stained fiber bundles or cell clusters were observed in the primary olfactory system. There were no GABA-ir cells that appeared at the same positions over preparations. To determine the number of GABA-ir cells in the primary olfactory system, we counted the cell bodies in all 16 sections obtained from a single well-stained inferior tentacle. A total of 592 GABA-ir cells were dentified in the sections, which included 526 cells (89%) in the digits, 18 cells (3%) in the cell masses, and 48 cells (8%) in the tentacular ganglion.

GABA-ir cells were also found in the CNS (Fig. 3). A single cell was found in the buccal ganglia (Fig. 3A). Neurons with small cell bodies aggregated into discrete clusters within the cerebral (Fig. 3B, C) and pedal ganglia (Fig. 3D). A fiber bundle was detected in the pedal commissure (Fig. 3D).

Distribution of AChE-containing neurons

AChE-containing fibers were detected in large neuropil areas of the primary olfactory system including the digits, tentacular ganglion, and tentacular nerve (Fig. 4). A large portion of neuropil of the digits was filled with AChE-stained fiber bundles with strong activity, and these fibers converged at the basal region of the digits (asterisks in Fig. 4A–C). A portion of the fibers coursed near the edge of tentacular ganglion (Fig. 4E) and entered the tentacular nerve (Fig. 4F).

AChE-stained cell bodies were also detected in the digits, cell masses, and tentacular ganglion (Fig. 5). Weakly stained sensory-like cells with sharp cell bodies (long axis, ~ 8 μm) were found in the digits just below the sensory epithelium, called lobule (Fig. 5A). A number of small cell bodies with the long axis of 3–7 μm in the digits (arrowhead in Fig. 5B), cell masses (arrowhead in Fig. 5C), and tentacular

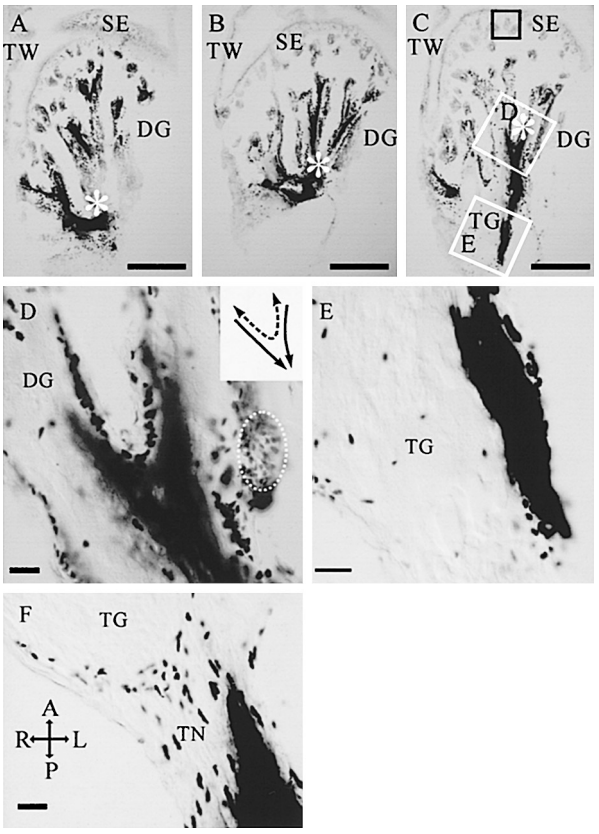

Fig. 4. AChE-containing fiber bundles in the digits and tentacular ganglion. A–C. Whole views of the stained fiber bundles in the digits. A serial-section of the left superior tentacle is shown from the dorsal to ventral side. The stained fibers converge at the branching sites (asterisks). The black line box in C is magnified in Fig. 5A, and the white line boxes in C are magnified in D and E. D. Magnified view of stained cell bodies and fiber bundles in the digits. Note the strong staining of most cell bodies and fiber bundles. Some lightly stained cell bodies (broken-lined circle) are also observed. Possible pathways of the fiber bundles are illustrated in the inset. The dotted line indicates fibers that connect adjacent branches. The solid line indicates fibers that extend into the tentacular ganglion. E. Magnified view of stained cell bodies and fiber bundles in the tentacular ganglion. F. Magnified view of stained cell bodies and fiber bundles in the tentacular nerve of the left superior tentacle. All sections of the tentacles are viewed from the ventral side. Calibration: A–C, 200 μm; D–F, 20 μm. SE, sensory epithelium; TW, tentacular wall; DG, digits; TG, tentacular ganglion; A, anterior; P, posterior; L, left; R, right; TN, tentacular nerve.

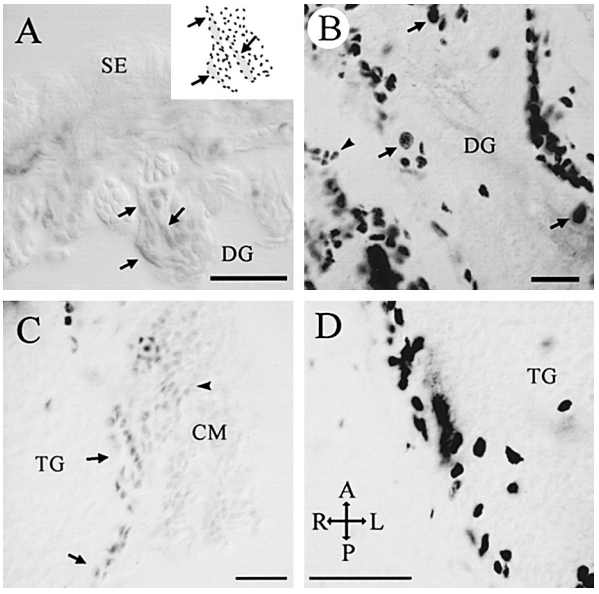

Fig. 5. AChE-containing cell bodies in the digits and tentacular ganglion. A. Stained neurons showing their processes traveling to the sensory epithelium of the left superior tentacle. Arrows point to the cell bodies. The black line box in Fig. 4C is magnified. Schematic drawing of the stained sensory-like neurons with sharp cell bodies are shown in the inset. B. Stained cells with large (arrows) and small (arrowhead) cell bodies in the digits of the right superior tentacle. Note in the same section the presence of small cells with strong and weak (arrowhead) staining. C. Stained cell bodies in the left cell mass of the right superior tentacle. Note the aggregation of stained cells in the inner layer of the cell mass. Arrowhead and arrows point to weakly-stained small cell bodies in the cell mass and tentacular ganglion, respectively. D. Stained cell bodies in the tentacular ganglion of the right superior tentacle. All sections of the tentacles are viewed from the ventral side. Calibration: 20 μm. SE, sensory epithelium; DG, digits; CM, cell mass; TG, tentacular ganglion; A, anterior; P, posterior; L, left; R, right.

ganglion (arrows in Fig. 5C) showed weak staining for AChE. Strong AChE staining was detected in a proportion of small cell bodies with long axis (3–7 μm) located in the cell layer of the digits (Fig. 5B) and tentacular ganglion (Fig. 5D). Some large cells with round (6 by 6 μm) or oval-shaped (long axis, > 8 μm) cell bodies showing strong activity were located in the cell layer of the digits (Fig. 5B). Aggregates of stained neurons were detected near the boundary between the tentacular ganglion and cell masses (Fig. 5C). To determine the proportion of each type of AChE-containing cells in the primary olfactory system, we counted the cell bodies using a representative section (15th of 21 sections counted from the dorsal side) from a well-stained superior tentacle. The representative section included sensory epithelium, digits, tentacular ganglion, and tentacular nerve. The total number of AChE-containing cells in this section was 2430. The counts of strongly and weakly stained cells were 468 (19.3%) and 1962 (80.7%), respectively. Uniform staining that was sufficiently strong to obscure the organelles within the cell body was considered “strong” staining. The numbers of stained cells with a large cell body (long axis, > 8 μm) and a round medium-sized cell body (6×6 μm) were 11 (0.5%) and 54 (2.2%), respectively. There were 2300 (94.7%) and 130 (5.3%) cells in the digits and tentacular ganglion, respectively.

AChE activity was also detected in the neuropil region of the cerebral ganglia but not that of the PC lobe (Fig. 6). Serial AChE-stained sections showed that the fiber bundle traveling in the tentacular nerve entered the neuropil of the cerebral ganglion, bypassed the neuropil of the PC lobe, and terminated in the metacerebrum (Fig. 6A–D). The stained small neurons in the cell masses of the right and left

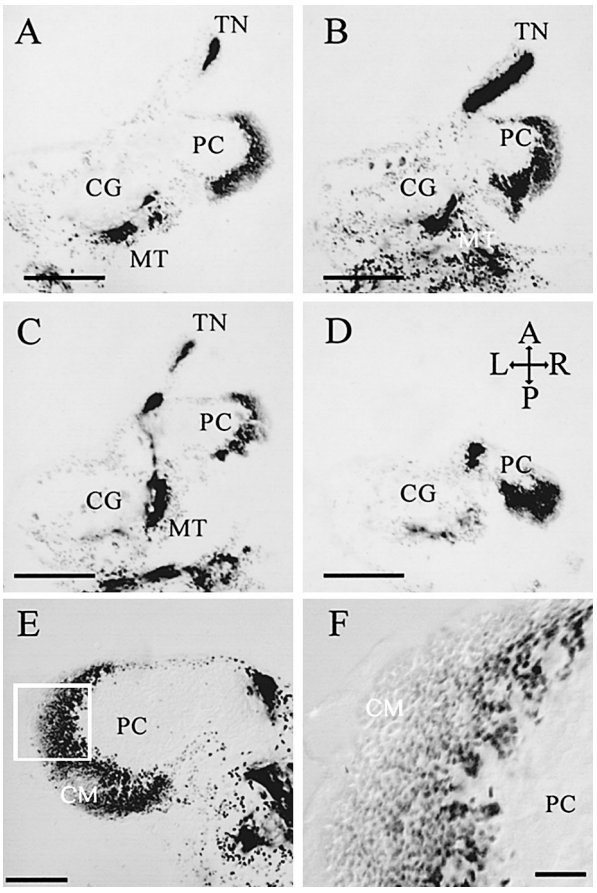

Fig. 6. AChE-containing cell bodies and fiber bundles in the cerebral ganglion. A–D. Serial sections of the cerebral ganglion. Note the entry of the fiber bundle into the metacerebrum of the cerebral ganglion but not the PC lobe. The cell mass of the right PC lobe displays AChE activity. E. Stained cell bodies in the cell mass in the left PC lobe. Neurons in the cell mass both in the right (A–D) and left PC lobes show strong staining. F. Magnified view of the right PC lobe in the box in E. Calibration: A–D, 200 μm; E, 100 μm; F, 20 μm. TN, tentacular nerve; PC, procerebral lobe; CG, cerebral ganglion; MT, metacerebrum; A, anterior; P, posterior; R, right; L, left; CM, cell mass.

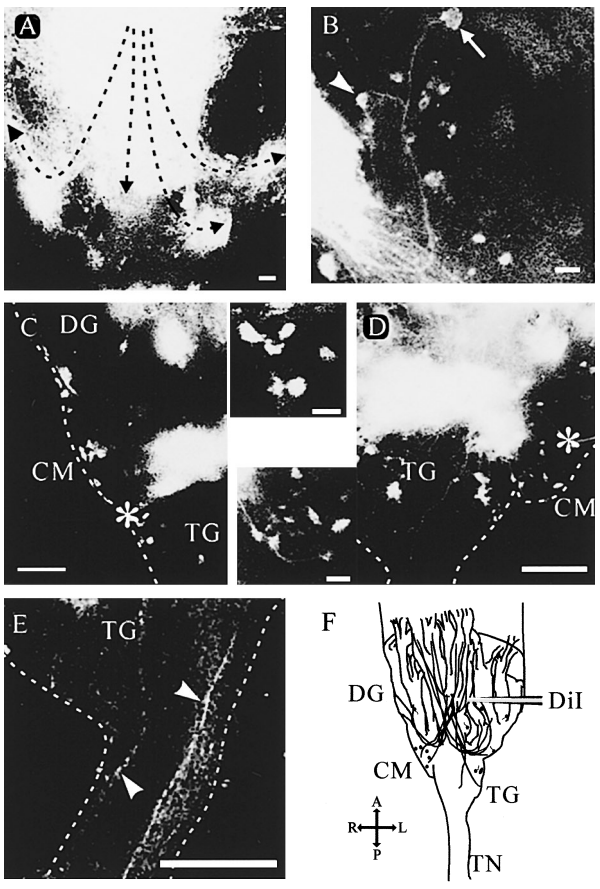

Fig. 7. Cell bodies and fibers stained by DiI crystals placed on the central group of the digits. A. Stained fibers turning into neighboring digits of the left inferior tentacle. Arrows indicate fibers running into adjacent branches. B. Stained cell with large (arrow) and small (arrowhead) cell bodies in the neighboring digits of the right inferior tentacle. The left group of the digits of the right inferior tentacle is shown. C. Stained cell bodies in the left side of the digits and cell mass and tentacular ganglion of the left inferior tentacle. The magnified view of the stained cell bodies in the tentacular ganglion (asterisk) is shown in the inset (top right). D. Stained cell bodies in the right side of the cell mass and the tentacular ganglion of the left inferior tentacle. The magnified view of stained cell bodies in the cell mass (asterisk) is shown in the inset (lower left). E. Stained fibers running into the tentacular nerve of the left inferior tentacle. Note the entry of two fibers into the tentacular nerve (arrowheads). F. Schematic drawing of stained cell bodies and fibers. All images were acquired using a confocal laser scanning microscope. All sections of the tentacles were viewed from the ventral side. The white broken-lines in C–E indicate the outlines of the preparations. Calibration: A–B, 20 μm; C–E, 100 μm. DG, digits; CM, cell mass; TG, tentacular ganglion; A, anterior; P, posterior; L, left; R, right.

PC lobes aggregated near the boundary between the neuropil and cell masses (Fig. 6E, F).

Distribution of cell bodies and fibers stained by DiI crystal

The above physiological and histological findings suggest that the primary olfactory system in *L. marginatus* houses interconnected networks, which include spatially separated sites in the digits and tentacular ganglion. To map these networks, we stained the neurons that had neurites (or cell bodies) passing through the central group of the digits by the vital staining with DiI crystal placed on that region. Several stained fibers filling the neuropil of the digits were observed (Fig. 7A). A considerable number of the stained fibers ran into neighboring branches of the digits (arrows in Fig. 7A). Large (long axis, 22 μm) and medium (long axis, 14 μm) DiI-stained cell bodies were found with their neurites traversing to neighboring branches (arrow and arrowhead in Fig. 7B). Stained cell bodies (long axis, 10–15 μm) were also found in the cell masses (Fig. 7C, D) and tentacular ganglion (asterisk in Fig. 7C). Some stained fibers entered the tentacular nerve (Fig. 7E). Fig. 7F summarizes schematically the distribution of DiI-stained fibers and cell bodies.

When the DiI crystals were placed on the cell masses, some stained fibers were observed in the digits, tentacular ganglion, and tentacular nerve (Fig. 8). The neuropil region

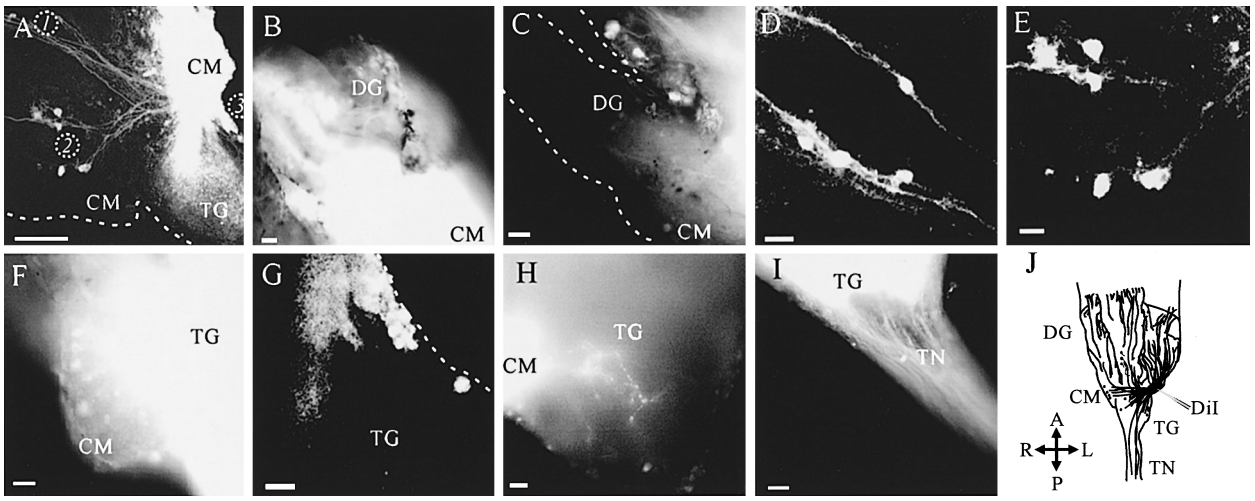

Fig. 8. Cell bodies and fibers stained by DiI crystals placed on the cell mass. A. Stained fibers in the digits and tentacular ganglion of the left inferior tentacle. DiI crystals were placed on the left cell mass. Stained fibers in the left, central and right groups of the digits are shown. Note that the ipsilateral side (left group) of the digits is the most strongly stained area. B. Stained fibers in the left group of the digits of the right superior tentacle. DiI crystals were placed on the left cell mass. The left group of the digits of this preparation was also filled with the stained fibers. C. Stained monopolar cells in the central group of the digits of the right superior tentacle. A monopolar cell with a small cell body is located near the branching region. DiI crystals were placed on the left cell mass. D. Magnified view of the stained bipolar cells in the central group of the digits. The position is marked by number *1* in A. These cells are bipolar and the distal ends ran into the tip of the digits. E. Magnified view of the stained cell bodies in the right group of the digits. The position is marked by number *2* in A. F. Stained cell bodies in the right cell mass of the right superior tentacle. DiI crystals were placed on the left cell mass. G. Magnified view of stained cell bodies in the tentacular ganglion. The position is marked by number *3* in A. H. Stained fibers with varicosities extending into the tentacular nerve in the tentacular ganglion of the left inferior tentacle. DiI crystals were placed on the right cell mass. I. Stained fiber bundles in the tentacular nerve of the right superior tentacle. DiI crystals were placed on the left cell mass. J. Schematic drawing of the stained cell bodies and fibers. Images were acquired using a confocal laser scanning microscope (A, D, E, G) and a cooled CCD camera (B, C, F, H, I). All sections of the tentacles are viewed from the ventral side. The white broken-lines in A, C, and G indicate the outlines of the preparations. Calibration: A, 100 μm; B-I, 20 μm. CM, cell mass; TG, tentacular ganglion; DG, digits; TN, tentacular nerve; A, anterior; P, posterior; L, left; R, right.

of the ipsilateral side of the digits was filled with stained fibers (Fig. 8A, B). The neuropil region of the tentacular ganglion was also filled with fine stained fibers (Fig. 8A). Stained cell bodies were observed in the digits (Fig. 8A, C–E), contralateral side of the cell mass (Fig. 8F), and tentacular ganglion (Fig. 8G). Bipolar DiI-stained cells with oval-shaped cell bodies (long axis, 12–15 μm) were found in the digits (Fig. 8D). The distal processes reached the tip of the digits. Medium cells with oval (long axis, ~ 9 μm) (Fig. 8C) and round (long axis, ~ 15 μm) (Fig. 8E) cell bodies were found in the digits. The stained cells in the cell mass (Fig. 8F) and tentacular ganglion (Fig. 8G) had smaller cell bodies (long axis, ~ 9 μm and 12 μm, respectively) than those in the digits. Neurites with varicosities were identified in the tentacular ganglion (Fig. 8H) and entering the tentacular nerve (Fig. 8I). We summarized schematically the distribution of DiI-stained fibers and cell bodies (Fig. 8J). These results showed that the primary olfactory system in *L. marginatus* houses highly interconnected networks.

DISCUSSION

The major findings of the present study on the primary olfactory system of the terrestrial slug *L. marginatus* were the recording of spatially coherent neural oscillations at 1–2 Hz generated by this system and the delineation of a complex and highly interconnected neural network containing GABAergic and cholinergic fibers. DiI staining also showed that the neurons in the three groups of the digits, cell masses, and tentacular ganglion were highly interconnected. These anatomic features suggest that the neural network serves the spatially coherent neural oscillations in the primary olfactory system.

GABAergic neurons in the primary olfactory system and CNS

Four types of neurons have been studied in the digits and tentacular ganglion by backfilling tentacular nerves with horseradish peroxidase in a snail (Chase and Kamil, 1983) and with Lucifer yellow in *L. marginatus* (Ito *et al.*, 2000). The four types of stained neurons were “sensory neurons”, “gamma cells”, “ganglion cells”, and “lateral cells”. The location and morphological features of the cell bodies of GABA-ir cells in the dermo-muscular sheaths of the tentacular wall (Fig. 2B) resembled those of the lateral cells, whose function is unknown. The distribution and morphological features of the cell bodies of the small GABA-ir cells found in the digits, cell mass, and tentacular ganglion resembled those of the ganglion cells. Although the lateral and ganglion cells send their neurites to the tentacular nerve, no GABA-ir fibers were detected in the tentacular nerve. Therefore, the GABA-ir neurons were considered to be local interneurons. Local

interneurons with a process ramifying within the neuropil of the digits were revealed by a double chromation method (Hernádi, 1982).

The distribution pattern of GABAergic cells in the CNS of *L. marginatus* detected in the present study is almost identical to that described previously in *L. maximus* (Cooke and Gelperin, 1988), and other mollusks such as *Helisoma* (Richmond *et al*., 1991) and *Helix* (Bravarenko *et al*., 2001). These studies reported the presence of cell bodies of GABAergic neurons in the buccal, cerebral and pedal ganglia. This is consistent with the results of the present study. Our study provides the first description of GABAergic neurons outside the CNS in mollusk.

AChE activity in the primary olfactory system and CNS

Our study is the first to describe the distribution of AChE-stained neural elements in the primary olfactory system of mollusks. We believe that some of these neurons are probably cholinergic neurons. Our results showed that the AChE-fiber bundle extended from the tip of the digits to the metacerebrum, but not the PC lobe, i.e., the olfactory center, via the tentacular nerve. In addition, the fiber bundle bypassed the center of the neuropil of the tentacular ganglion where synaptic contacts between olfactory neurons and secondary neurons occur (Chase and Tolloczko, 1993). Because the tentacles are not only olfactory organs but also mechanosensory organs, these fibers may transmit mechanosensory inputs to the brain. Indeed, putative cholinergic mechanosensory fibers were detected in the antennal nerve of sphinx moth *Manduca sexta* by a similar histochemical method, and they were found to bypass the antennal lobe and project to the antennal mechanosensory and motor center of the deutocerebrum (Homberg *et al*., 1995).

The distribution of AChE-containing cells in the tentacular ganglion resembled that in the PC lobe. Only the deep regions of the cell masses, both in the tentacular ganglion and the PC lobe, showed AChE activity. Neurons with varicosities were found in the PC lobe (Wang *et al*., 2001) as well as in the cell mass in the present study (Fig. 8H). Interestingly, one embryological study showed that the PC lobe shares its early development with the tentacular ganglion and joins the cerebral ganglion at a relatively late stage (Van Mol, 1967). This may explain the similarity between the two regions with regard to the distribution of AChE-containing cells.

Cells connecting the digits, cell masses and tentacular ganglion

Because most of the DiI-stained cells had larger cell bodies (long axis, > 9 μm) than ganglion cells (long axis, 4–8 μm), which formed the majority of cells of the digits and tentacular ganglion (Ito *et al*., 2000), they are considered to be gamma cells. Because these gamma cells were present in both the digits and the cell mass, we considered that they connect these regions to each other. They also connect with the neighboring groups of the digits. Another possible cell type that connects the neighboring groups of the digits is the small GABA-ir cells (Fig. 2C, F). Based on the shape and length of cell body, these cells are considered to be ganglion cells. Indeed, we did not detect large cell bodies immunoreactive to GABA. Unfortunately, we did not identify the cell body of each AChE-containing fiber that turned into the neighboring branches of the digits.

We have recently reported that GABA and ACh decreased the amplitude of spontaneous oscillations in the tentacular nerve (Ito *et al*., 2003a). Therefore, it is conceivable that GABAergic and putative cholinergic networks identified in the present study are involved in the oscillatory circuits. Odor stimuli typically produce a decrease in the amplitude of tentacular nerve activity (Ito *et al*., 2001), which correlates with odor-evoked spike generation (Ito *et al*., 2003b). Since the oscillatory behavior is a common feature of the olfactory systems of the vertebrates (Adrian, 1950; Ottoson, 1959; Dorries and Kauer, 2000; Nikonov *et al*., 2002) and invertebrates (Gelperin and Tank, 1990; Laurent, 1997; Stopfer *et al*., 1997), it is important to understand such behavior for a full assessment of the olfactory process.

We conclude that the primary olfactory system of the terrestrial slug *L. marginatus* contains highly interconnected neural circuits serving the spatially coherent neural oscillations at 1–2 Hz. Such oscillatory network may include GABAergic and putative cholinergic fibers. Our study provides the basic structure of the olfactory neural circuit in the primary olfactory system of the terrestrial slugs.

ACKNOWLEDGMENTS

This work was supported in part by research fellowships (Nos. 05725 and 00169) from the Japan Society for the Promotion of Science for Young Scientists to I.I. and by a Grant-in-Aid (No. 14540622) from the Japan Society for the Promotion of Science and grants from the Yamada Science Foundation, the Itoh Science Foundation, and the Kato Memorial Bioscience Foundation to E.I.

REFERENCES

Adrian ED (1950) The electrical activity of the mammalian olfactory bulb. Electroencephalogr Clin Neurophysiol 2: 377–388

Bravarenko NI, Ierusalimsky VN, Korshunova TA, Malyshev AY, Zakharov IS, Balaban PM (2001) Participation of GABA in establishing behavioral hierarchies in the terrestrial snail. Exp Brain Res 141: 340–348

Chase R, Kamil R (1983) Neuronal elements in snail tentacles as revealed by horseradish peroxidase backfilling. J Neurobiol 14: 29–42

Chase R, Tolloczko B (1993) Tracing neural pathways in snail olfaction: From the tip of the tentacles to the brain and beyond. Microsco Res Tech 24: 214–230

Cooke IR, Gelperin A (1988) Distribution of GABA-like immunoreactive neurons in the slug *Limax maximus*. Cell Tissue Res 253: 77–81

Dorries KM, Kauer JS (2000) Relationships between odor-elicited oscillations in the salamander olfactory epithelium and olfactory bulb. J Neurophysiol 83: 754–765

Delaney KR, Gelperin A, Fee MS, Flores JA, Gervais R, Tank DW, Kleinfeld D (1994) Waves and stimulus-modulated dynamics in

an oscillating olfactory network. Proc Natl Acad Sci USA 91: 669–673

Fujie S, Aonuma H, Ito I, Gelperin A, Ito E (2002) The nitric oxide/cyclic GMP pathway in the olfactory processing system of the terrestrial slug *Limax marginatus*. Zool Sci 19: 15–26

Gelperin A, Flores J (1997) Vital staining from dye-coated microprobes identifies new olfactory interneurons for optical and electrical recording. J Neurosci Methods 72: 97–108

Gelperin A, Tank DW (1990) Odour-modulated collective network oscillations of olfactory interneurons in a terrestrial mollusc. Nature 345: 437–440

Hatakeyama D, Ito I, Ito E (2001) Complement receptor 3-like immunoreactivity in the superior and inferior tentacles of terrestrial slug, *Limax marginatus*. Zool Sci 18: 5–10

Hernádi L (1982) Organization of sensory pathways in the anterior tentacle of *Helix pomatia* L. A light microscopic study. Z Mikrosk Anat Forsch 96: 695–703

Homberg U, Hoskins SG, Hildebrand JG (1995) Distribution of acetylcholinesterase activity in the deutocerebrum of the sphinx moth *Manduca sexta*. Cell Tissue Res 279: 249–259

Inokuma Y, Inoue T, Watanabe S, Kirino Y (2002) Two types of network oscillations and their odor responses in the primary olfactory center of a terrestrial mollusk. J Neurophysiol 87: 3160–3164

Ito I, Kimura T, Ito E (2001) Odor responses and spontaneous oscillatory activity in tentacular nerves of the terrestrial slug, *Limax marginatus*. Neurosci Lett 304: 145–148

Ito I, Kimura T, Suzuki H, Sekiguchi T, Ito E (1999) Effects of electrical stimulation of the tentacular digits of a slug upon the frequency of electrical oscillations in the procerebral lobe. Brain Res 815: 121–125

Ito I, Nakamura H, Kimura T, Suzuki H, Sekiguchi T, Kawabata K, Ito E (2000) Neuronal components of the superior and inferior tentacles in the terrestrial slug, *Limax marginatus*. Neurosci Res 37: 191–200

Ito I, Kimura T, Watanabe S, Kirino Y, Ito E (2003a) Modulation of two oscillatory networks in the peripheral olfactory system by γ-aminobutyric acid, glutamate and acetylcholine in the terrestrial slug *Limax marginatus*. J Neurobiol (in press)

Ito I, Watanabe S, Kimura T, Kirino Y, Ito E (2003b) Negative relationship between odor-induced spike activity and spontaneous oscillations in the primary olfactory system of the terrestrial slug *Limax marginatus*. Zool Sci 20: 1327–1335

Iwama A, Yabunaka A, Kono E, Kimura T, Yoshida S, Sekiguchi T (1999) Properties of wave propagation in the oscillatory neural network in *Limax marginatus*. Zool Sci 16: 407–416

Kimura T, Toda S, Sekiguchi T, Kirino Y (1998) Behavioral modulation induced by food odor aversive conditioning and its influence on the olfactory responses of an oscillatory brain network in the slug *Limax marginatus*. Learn Mem 4: 365–375

Laurent G (1997) Olfactory processing: Maps, Time and Codes. Cur Opin Neurobiol 7: 547–553

Nikonov AA, Parker JM, Caprio J (2002) Odorant-induced olfactory receptor neural oscillations and their modulation of olfactory bulbar responses in the channel catfish. J Neurosci 22: 2352–2362

Ottoson D (1959) Comparison of slow potentials evoked in the frog's nasal mucosa and olfactory bulb by natural stimulation. Acta Physiol Scand 47: 149–159

Richmond JE, Bulloch AGM, Bauce L, Lukowiak K (1991) Evidence for the presence, synthesis, immunoreactivity, and uptake of GABA in the nervous system of the snail *Helisoma trivolvis*. J Comp Neurol 307: 131–143

Rubakhin SS, Szücs, Rózsa KS (1996) Characterization of the GABA response on identified dialysed *Lymnaea* neurons. Gen Pharmac 27: 731–739

Stopfer M, Bhagavan S, Smith BH, Laurent G (1997) Impaired odour discrimination on desynchronization of odour-encoding neural assemblies. Nature 390: 70–74

Tago H, Kimura H, Maeda T (1986) Visualization of detailed acetylcholinesterase fiber and neuron staining in rat brain by a sensitive histochemical procedure. J Histochem Cytochem 34: 1431–1438

Van Mol JJ (1967) Étude morphologique et phylogénétique du ganglion céréboîde des Gastéropodes Pulmonés (Mollusques). Mém Acad R Belg (Classe Sci) 37: 1–168

Wang JW, Denk W, Flores J, Gelperin A (2001) Initiation and propagation of calcium-dependent action potentials in a coupled network of olfactory interneurons. J Neurophysiol 85: 977–985

Watanabe S, Inoue T, Murakami M, Inokuma Y, Kawahara S, Kirino Y (2001) Modulation of oscillatory neural activities by cholinergic activation of interneurons in the olfactory center of a terrestrial slug. Brain Res 896: 30–35

(Received July 1, 2003 / Accepted August 11, 2003)